

# Evaluation of $^{68}\text{Ga}$ -DOTA-TOC PET/CT for the detection of duodenopancreatic neuroendocrine tumors in patients with MEN1

Clément Morgat<sup>1,2,3</sup> · Fritz-Line Vélayoudom-Céphise<sup>4</sup> · Paul Schwartz<sup>3</sup> · Martine Guyot<sup>3</sup> · Delphine Gaye<sup>5</sup> · Delphine Vimont<sup>1,2</sup> · Jürgen Schulz<sup>1,2</sup> · Joachim Mazère<sup>1,2,3</sup> · Marie-Laure Nunes<sup>4</sup> · Denis Smith<sup>6</sup> · Elif Hindić<sup>1,2,3</sup> · Philippe Fernandez<sup>1,2,3</sup> · Antoine Tabarin<sup>4</sup>

Received: 19 October 2015 / Accepted: 15 January 2016  
© Springer-Verlag Berlin Heidelberg 2016

## Abstract

**Context** Somatostatin receptor scintigraphy with  $^{111}\text{In}$ -pentetretotide (SRS) is used to detect duodenopancreatic neuroendocrine tumors (dpNETs) in multiple endocrine neoplasia type 1 (MEN1). However, SRS has limited sensitivity for this purpose. Positron emission tomography/computed tomography (PET/CT) with  $^{68}\text{Ga}$ -DOTA-TOC has a higher rate of sporadic dpNETs detection than SRS but there is little data for dpNETs detection in MEN1.

**Purpose** To compare the performances of  $^{68}\text{Ga}$ -DOTA-TOC PET/CT, SRS and contrast-enhanced computed tomography (CE-CT) to diagnose dpNETs in MEN1.

**Design and setting** Single-institution prospective comparative study

**Patients and methods** Nineteen consecutive MEN1 patients (aged  $47 \pm 13$  years) underwent  $^{68}\text{Ga}$ -DOTA-TOC PET/CT, SRS, and CE-CT within 2 months in random order. Blinded

readings of images were performed separately by experienced physicians. Unblinded analysis of CE-CT, combined with additional magnetic resonance imaging, endoscopic-ultrasound,  $^{18}\text{F}$ -2-fluoro-deoxy-D-glucose ( $^{18}\text{F}$ -FDG) PET/CT or histopathology results served as reference standard for dpNETs diagnosis.

**Results** The sensitivity of  $^{68}\text{Ga}$ -DOTA-TOC PET/CT, SRS, and CE-CT was 76, 20, and 60 %, respectively ( $p < 0.0001$ ). All the true-positive lesions detected by SRS were also depicted on  $^{68}\text{Ga}$ -DOTA-TOC PET/CT.  $^{68}\text{Ga}$ -DOTA-TOC PET/CT detected lesions of smaller size than SRS ( $10.7 \pm 7.6$  and  $15.2 \pm 5.9$  mm, respectively,  $p < 0.03$ ). False negatives of  $^{68}\text{Ga}$ -DOTA-TOC PET/CT included small dpNETs ( $< 10$  mm) and  $^{18}\text{F}$ -FDG PET/CT positive aggressive dpNETs. No false positives were recorded. In addition, whole-body mapping with  $^{68}\text{Ga}$ -DOTA-TOC PET/CT identified extra-abdominal MEN1-related tumors including one

---

Clément Morgat and Fritz-Line Vélayoudom-Céphise are both first co-authors.

---

Philippe Fernandez and Antoine Tabarin contributed equally to this work.

---

✉ Clément Morgat  
clement.morgat@chu-bordeaux.fr

Fritz-Line Vélayoudom-Céphise  
flcephise@gmail.com

<sup>1</sup> CNRS, INCIA, UMR 5287, 33000 Bordeaux, France

<sup>2</sup> University of Bordeaux, INCIA, UMR 5287, 33000 Bordeaux, France

<sup>3</sup> Department of Nuclear Medicine, University Hospital of Bordeaux, 33000 Bordeaux, France

<sup>4</sup> Department of Endocrinology, USN Haut-Lévêque, 33604 Pessac, France

<sup>5</sup> Department of Radiology, University Hospital of Bordeaux, 33604 Pessac, France

<sup>6</sup> Department of Oncology, University Hospital of Bordeaux, 33000 Bordeaux, France

neuroendocrine thymic carcinoma identified by the three imaging procedures, one bronchial carcinoid undetected by CE-CT and three meningiomas undetected by SRS.

**Conclusions** Owing to higher diagnostic performance,  $^{68}\text{Ga}$ -DOTA-TOC PET/CT (or alternative  $^{68}\text{Ga}$ -labeled somatostatin analogues) should replace  $^{111}\text{In}$ -pentetreotide in the investigation of MEN1 patients.

**Keywords** Duodenopancreatic neuroendocrine tumors · Multiple endocrine neoplasia type 1 ·  $^{68}\text{Ga}$ -DOTA-TOC PET/CT ·  $^{111}\text{In}$ -pentetreotide SPECT/CT · Contrast-enhanced computed tomography

## Introduction

Multiple endocrine neoplasia type 1 (MEN1) is an autosomal dominant hereditary syndrome caused by germline mutations of the *menin* tumor suppressor gene [1]. MEN1 is responsible for various endocrine and non-endocrine tumors amongst which parathyroid adenoma/hyperplasia, duodenopancreatic neuroendocrine tumors (dpNETs), and pituitary adenomas are the more prevalent [2]. Amongst dpNETs, non-functioning tumors (NF) are the most common, followed by gastrinomas and insulinomas [3]. dpNETs have malignant potential and MEN1 prognosis is mainly linked to their metastatic risk [4, 5]. Since surgery is the only curative treatment, systematic detection and follow-up of dpNETs are warranted in MEN1 patients [3]. Given that MEN1-associated dpNETs are frequently multiple, their accurate diagnosis presents significant challenges [3]. Various imaging procedures have been proposed for this purpose such as  $^{111}\text{In}$ -pentetreotide-labeled somatostatin receptor scintigraphy (SRS), endoscopic ultrasound (EUS), contrast-enhanced-computed tomography (CE-CT) and magnetic resonance imaging (MRI). However, to date, no consensus for optimum radiological imaging in MEN1 patients has been established [3, 6].

SRS takes advantage of a unique feature of dpNETs: in 70–90 % of cases they exhibit expression of somatostatin receptor type 2 (SSTR<sub>2</sub>) [7]. However, the sensitivity of this functional imaging has limitations due to its low spatial resolution and inability to detect dpNETs with low SSTR density and/or small size [8]. Recently, some high affinity somatostatin analogs holding a DOTA-chelate and radiolabeled with  $^{68}\text{Ga}$  for PET/CT imaging have emerged, which supersede in resolution and sensitivity conventional SRS in the detection of metastatic or small neuroendocrine tumors [7–10].

To date, only a few studies have evaluated the performance of the new somatostatin receptor PET tracers for detection of dpNETs in MEN1 patients. However, two were retrospective studies that did not include comparison with SRS and multi-phase CE-CT [11, 12] and two were prospective studies using  $^{68}\text{Ga}$ -DOTA-Tyr<sup>3</sup>-Octreotate ( $^{68}\text{Ga}$ -DOTA-TATE) PET/CT

[13, 14]. The aim of our study was therefore to compare prospectively the performance of  $^{68}\text{Ga}$ -DOTA-Tyr<sup>3</sup>-octreotide ( $^{68}\text{Ga}$ -DOTA-TOC) PET/CT, SRS, and CE-CT for the diagnosis of dpNETs in MEN1 patients.

## Patients and methods

### Patients

Nineteen genetically confirmed MEN1 patients (12 women, age at inclusion:  $47 \pm 13$  years, range, 26–70 years), previously evaluated and treated in our department, were enrolled in this prospective study (Clinical Trial GALTEP, Eudract 2013-003927-12). Patients were recruited consecutively during their scheduled follow-up. Written informed consent was obtained from all individual participants included in the study that was approved by the local ethical committee.

All patients had primary hyperparathyroidism, 12 were treated for pituitary adenomas, two underwent resection of lung neuroendocrine tumors (NETs), and one underwent resection of bilateral adrenal carcinomas. Endoscopic enucleations were previously performed for two insulinomas (P1, P12), one pancreatic gastrinoma (P18) while a distal pancreatectomy was performed for a NF dpNET (P14) and a pancreatic gastrinoma (P7). Five patients were successfully treated with proton pump inhibitors for Zollinger–Ellison syndrome (ZES) at the time of the study (P4, P7, P10, P18, P19). In the remaining asymptomatic patients, systematic measurement of circulating gut hormones revealed an increased plasma concentration of pancreatic polypeptide in two patients (371 and 235 pmol/l, normal value < 100 pmol/l; P3 and P17, respectively). Clinical features of the 19 MEN1 patients are summarized in Table 1.

### $^{68}\text{Ga}$ -DOTA-TOC radiosynthesis

Gallium-68 was obtained from a  $^{68}\text{Ge}/^{68}\text{Ga}$  generator (IASON, Obninsk, Russia) and complexed with DOTA-TOC (ABX GmbH; ~50  $\mu\text{g}$ , Garching, Germany) using microwaves (90 °C, 5 min) as previously described [15]. After sterile filtration, all radiopharmaceutical preparations were checked for activities [16], radiochemical purity, specific activity, volume, and sterility. Care was taken that all radiopharmaceutical preparations contained 1.5 MBq/kg and maximum 50  $\mu\text{g}$  of  $^{68}\text{Ga}$ -DOTA-TOC for each patient.  $^{68}\text{Ga}$ -DOTA-TOC preparations were obtained with radiochemical purities > 95 % and specific activities of  $8.3 \pm 5.6$  GBq/ $\mu\text{mol}$ .  $^{68}\text{Ga}$ -DOTA-TOC was intravenously injected (mean,  $97.1 \pm 13.3$  MBq, 20.9  $\mu\text{g}$ ; median 98.2 MBq, 20.5  $\mu\text{g}$ ; range, 74.6–124.3 MBq, 5.7–34  $\mu\text{g}$ ).

**Table 1** Clinical features of MEN1 patients

Patient number	Sex	Age at diagnosis	Age at inclusion	Associated MEN1 lesions*	Previous pancreatic surgery	Complementary imaging
P1	F	43	45	1	Yes (insulinoma)	Yes Abdominal MRI
P2	M	52	66	1,2	No	Yes Abdominal MRI, <sup>18</sup> F-FDG PET/CT
P3	M	22	30	1,3	No	Yes Abdominal MRI, EUS
P4	F	26	37	1	No	Yes Abdominal MRI, EUS
P5	F	29	40	1,2	No	Yes Abdominal MRI
P6	F	39	45	1,2,4	No	Yes Abdominal and brain MRI, <sup>18</sup> F-FDG PET/CT
P7	F	32	39	1,2,5	Yes (gastrinoma)	Yes Abdominal MRI, EUS
P8	M	58	64	1	No	Yes EUS
P9	F	48	55	1,2	No	No
P10	M	29	44	1,3	No	No
P11	F	15	52	1,2	No	Yes Abdominal MRI, EUS
P12	F	17	26	1	Yes (insulinoma)	Yes Abdominal MRI, EUS, <sup>18</sup> F-FDG PET/CT
P13	F	18	36	1,2	No	No
P14	F	55	58	1	Yes (NF)	No
P15	M	11	31	1,2	No	No
P16	F	50	63	1,2,4	No	No
P17	F	27	54	1,2,4	No	Yes Abdominal MRI
P18	M	55	70	1,2	Yes (gastrinoma)	Yes Abdominal MRI
P19	M	14	45	1,2	No	Yes Abdominal and brain MRI, EUS, bronchial endoscopy

P patient, F female, M male, NF non-functioning, ZES Zollinger–Ellison syndrome

\* 1: primary hyperparathyroidism, 2: pituitary adenoma, 3: lung neuroendocrine tumor, 4: non-secreting adrenal nodules, 5: bilateral adrenal carcinoma

### <sup>68</sup>Ga-DOTA-TOC PET/CT imaging

All <sup>68</sup>Ga-DOTA-TOC examinations were performed on a dedicated scanner (Discovery RX, General Electric Medical System, Milwaukee, WI, USA), 60 min after injection in 3D mode. Care-dose sure CT scans for attenuation correction were acquired (80 mA, 140 kV, a 256 × 256 matrix, 3-mm slice thickness). The PET imaging sequence encompassed multiple bed position whole-body scans from the top of the skull to the proximal thighs (180 s each bed position). Iterative

reconstruction was performed with a scatter correction using the ordered subset expectation maximization technique (OSEM) with two iterations and 21 subsets. Reconstruction of PET images used corrections for attenuation, dead-time, random events, and scatter.

### SRS

<sup>111</sup>In-pentetreotide was prepared with the commercially available kit (Octreoscan, Covidien Imaging, Élancourt, France)

according to manufacturer instructions. Mean injected activity was  $149.5 \pm 4.9$  MBq. Whole-body imaging (speed 8 cm/min) was performed at 6 h after injection with a dual-detector scintillation camera (Symbia T2 Siemens, Erlangen, Germany or Discovery NM/CT 670 pro, General Electric Medical System, Milwaukee, WI, USA) equipped with a medium-energy parallel-hole collimator. Two 15-min planar images were recorded at 24 h, on cranial-thoracic and abdominal regions. Single photon-emission computed tomography/computed tomography (SPECT/CT) images of the abdomen were routinely performed at 24 h using the following parameters: rotation detection head,  $2 \times 180^\circ$ ;  $2 \times 64$  projections; 50 s per projection;  $128 \times 128$  matrix). Image reconstruction was performed by iterative flash 3D algorithm (14 iterations, eight subsets) on data acquired with Symbia T2 system, and by iterative OSEM algorithm (two iterations, ten subsets) on data acquired with Discovery system. Reconstruction procedure included attenuation correction (based on the CT maps) and scatter correction.

### CE-CT

Helical CT images of the neck, thorax, and abdomen were acquired with the SOMATOM Definition scanner (Siemens) with the following parameters: tube current, 120 kV; tube voltage: with “care dose” adaptation; reconstruction orientation, transverse; reconstruction section thickness, 2 mm. Typically, 2 ml/kg iohexol contrast media (Omnipaque 300; GE Healthcare) was administered with scan delays of 30 s for the arterial phase and 70 s for the portal phase. Images were reconstructed with a soft-tissue kernel B20f for arterial phase and B30f for portal phase.

### Imaging analysis

$^{68}\text{Ga}$ -DOTA-TOC PET/CT, SRS, and CE-CT were performed within 2 months. Two experienced nuclear medicine physicians aware of the MEN1 diagnosis but blinded to the results of morphological imaging, interpreted separately  $^{68}\text{Ga}$ -DOTA-TOC PET/CT and SRS SPECT/CT in a random fashion while an experienced radiologist performed blinded readings of CE-CT imaging. Criteria for image interpretation of  $^{68}\text{Ga}$ -DOTA-TOC PET/CT and SRS were based on visual analysis. In PET imaging, focally increased uptake, compared to that of the surrounding tissue, was read as positive. Diffuse uptake over the uncinatus process was considered physiological. For SRS analysis, increased uptake was assessed by comparison with uptake by liver tissue, according to the European Association of Nuclear Medicine recommendations [17].

Then, a collective and joint unblinded analysis of the  $^{68}\text{Ga}$ -DOTA-TOC PET/CT, SRS, and CE-CT was performed for each patient by the three physicians. When the results were discordant, complementary investigations by MRI, EUS,  $^{18}\text{F}$ -

FDG PET, or histology were performed on an individual basis to confirm (or not) the anatomical substratum of pathological findings on CE/CT or nuclear procedures. The combination of the unblinded analysis of the CE-CT with the complementary investigations results served as reference standard.

### Statistical analyses

Continuous data were expressed in mean  $\pm$  standard deviation. Categorical data were expressed in number and percentage. Sensitivity of  $^{68}\text{Ga}$ -DOTA-TOC PET/CT, SRS, and CE-CT for dpNETs detection were calculated on a per-lesion analysis. Chi-square test, non-parametric Kruskal–Wallis ANOVA and Mann–Whitney test were performed when indicated. A  $p$  value  $< 0.05$  was considered significant. Data analyses were performed using GraphPad software (La Jolla, CA, USA).

## Results

### Detection of duodenopancreatic neuroendocrine tumors (Table 2)

Seventy-five dpNETs were diagnosed using the reference standard (see above imaging analysis paragraph)(size:  $10.4 \pm 7.3$  mm; range, 2–45 mm): 59 were located in the pancreas (size:  $10.7 \pm 7.7$  mm; range, 2–45 mm), six in the duodenum (size:  $3.0 \pm 3.5$  mm; range, 3–13 mm), eight were lymph nodes (LN) on the lymphatic pathway of dpNETs (size:  $11.0 \pm 6.8$  mm; range, 2–25 mm) and two were liver metastases of 12 and 19 mm in size of a dpNET (P6).

In a per-lesion-analysis,  $^{68}\text{Ga}$ -DOTA-TOC PET/CT, SRS, and CE-CT depicted 57, 17, and 47 lesions, respectively. Among the 57 lesions described using  $^{68}\text{Ga}$ -DOTA-TOC PET/CT, all were true positive (TP) (size:  $10.7 \pm 7.6$  mm; range, 2–45 mm). No false positives (FP) of  $^{68}\text{Ga}$ -DOTA-TOC PET/CT were reported. Fifteen of the 17 lesions described using SRS were TP (size:  $15.2 \pm 5.8$  mm; range, 6–

**Table 2** Results of  $^{68}\text{Ga}$ -DOTA-TOC PET/CT, SRS and CE-CT for the detection of dpNETs: per-lesion analysis

	TP	TN	FP	FN	Sensitivity (%)	Specificity (%)
$^{68}\text{Ga}$ -DOTA-TOC PET/CT	57	4	0	18	76	100
SRS	15	2	2	60	20	50
CE-CT	45	2	2	30	60	50
$p$ value					$< 0.0001$	$< 0.01$

PET/CT positron emission tomography/computed tomography, SRS scintigraphy with  $^{111}\text{In}$ -pentetreotide, CE-CT contrast-enhanced computed tomography, TP true positive, TN true negative, FP false positive, FN false negative

25 mm) and two were FP, which corresponded to physiological uptake of the pancreatic uncus. Forty-five of 47 lesions identified by CE-CT were TP (size:  $11.9 \pm 8.2$  mm; range, 2–45 mm) and two were FP corresponding to intraductal papillary mucinous neoplasm (IPMN). Thus, the sensitivity of  $^{68}\text{Ga}$ -DOTA-TOC PET/CT, SRS and CE-CT for the detection of dpNETs differed significantly (76, 20, and 60 %, respectively,  $p < 0.0001$ ) (Table 2). The specificity of  $^{68}\text{Ga}$ -DOTA-TOC PET/CT, SRS, and CE-CT was 100, 50, and 50 %, respectively ( $p < 0.01$ ) (Tables 2 and 3).

### Comparison of $^{68}\text{Ga}$ -DOTA-TOC PET/CT and SRS

Fifteen concordant lesions were TP identified with  $^{68}\text{Ga}$ -DOTA-TOC PET/CT and SRS in 13 patients. Importantly, 42 dpNETs depicted in 18 patients by  $^{68}\text{Ga}$ -DOTA-TOC PET/CT were not seen using SRS (Fig. 1). Conversely, all the TP of SRS were described with  $^{68}\text{Ga}$ -DOTA-TOC PET/CT. The dpNETs identified with  $^{68}\text{Ga}$ -DOTA-TOC PET/CT were smaller than those identified with SRS ( $10.7 \pm 7.6$  and  $15.2 \pm 5.9$  mm, respectively,  $p < 0.03$ ). Incidentally, in patients treated by proton pump inhibitors,  $^{68}\text{Ga}$ -DOTA-TOC PET/CT identified five probable SRS negative gastrinomas located within the duodenum or periduodenal LN. The two FP of SRS were identified as physiological uptake of the pancreatic uncus with  $^{68}\text{Ga}$ -DOTA-TOC PET/CT.

### Comparison of $^{68}\text{Ga}$ -DOTA-TOC PET/CT and CE-CT

Thirty-two concordant TP dpNETs were identified with  $^{68}\text{Ga}$ -DOTA-TOC PET/CT and CE-CT in 16 patients. Twenty-five

dpNETs were identified with  $^{68}\text{Ga}$ -DOTA-TOC PET/CT and not seen with CE-CT. Interestingly, unblinded re-analysis of CE-CT images guided by the results of  $^{68}\text{Ga}$ -DOTA-TOC PET/CT disclosed 15 of the 25 dpNETs that were not identified during blinded analysis of CE-CT. These were three lesions of the pancreatic tail (3–24 mm in size), four lesions of the pancreatic body (3–11 mm in size), two lesions of the pancreatic head (each of 6 mm in size), four duodenal lesions (3–8 mm in size) and two peripancreatic LN (2 and 7 mm in size). The ten remaining lesions not seen with CE-CT were four lesions of the pancreatic head (4–5 mm), four lesions of the body (6–17 mm), and two lesions of the tail (5–17 mm).

Thirteen false negatives (FN) of  $^{68}\text{Ga}$ -DOTA-TOC PET/CT were identified by CE-CT and corresponded to ten pancreatic tumors (2–12 mm in size,  $5.3 \pm 1.0$  mm) in 11 patients, one peripancreatic metastatic LN of 25 mm in size, and two liver metastases of a grade 3 pancreatic NET (P6). These three last lesions displayed intense uptake during  $^{18}\text{F}$ -FDG PET/CT.

Complementary imaging performed to verify  $^{68}\text{Ga}$ -DOTA-TOC PET/CT images unseen with SRS and CE-CT, identified five additional lesions in P12 that were not seen with  $^{68}\text{Ga}$ -DOTA-TOC PET/CT nor CE-CT. These included one lesion of the pancreatic head (5 mm in size), two rapidly growing lesions of the tail (8 and 16 mm in size) and two peripancreatic LN (12 and 13 mm in size). These results warranted an evaluation with  $^{18}\text{F}$ -FDG PET/CT that showed an intense uptake of the lesions of the pancreatic tail and associated LN (Fig. 2). Three patients had confirmation of three lesions depicted by  $^{68}\text{Ga}$ -DOTA-TOC PET/CT: thymic confirmation in P2, well differentiated NET in P3, and typical carcinoid bronchial neuroendocrine tumor.

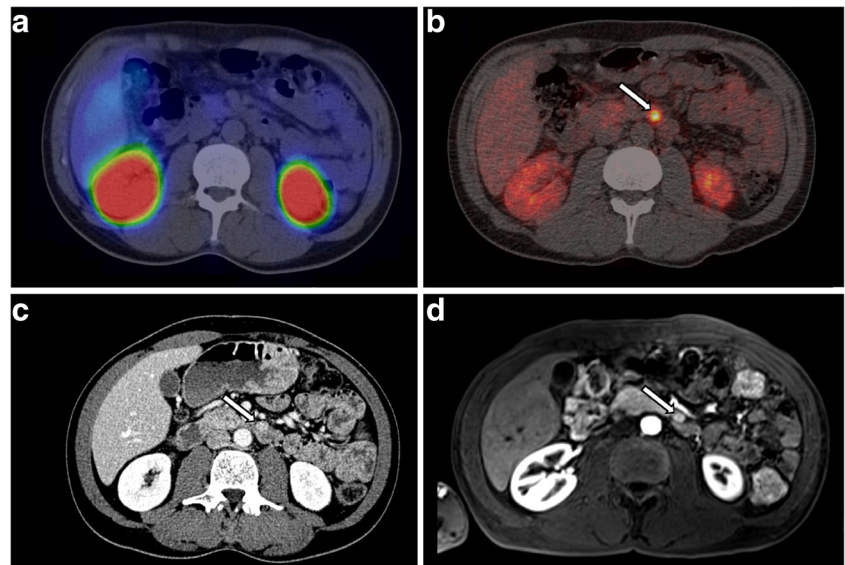
**Table 3** Organ-related findings according to unblinded analysis of imaging procedures

Lesion localization	$^{68}\text{Ga}$ -DOTA-TOC PET/CT	SRS	CE-CT
Pancreas lesions	46	11	37
- Head	11 [2–22]*	4 [7–22]	9 [2–22]
- Isthmus	3 [7–18]	1 [18]	4 [5–18]
- Body	13 [9–25]	2 [22–25]	7 [6–25]
- Body/tail junction	4 [7–14]	2 [14]	4 [7–14]
- Tail	13 [3–45]	1 [23]	11 [3–45]
- Uncus	2 [11–12]	1 [12]	2 [11–12]
Lymph nodes	5 [2–14]	2 [8–14]	4 [8–25]
Duodenum	6 [3–13]	2 [6–13]	2 [9–13]
Lung	1	1	0
Thymus	1	1	1
Brain	3	0	NS
Liver metastasis	0	0	2
Total of positive lesions	62	17	46
Total of invaded organs	6	5	5

NS non-suitable, PET/CT positron emission tomography/computed tomography, SRS scintigraphy with  $^{111}\text{In}$ -pentetreotide, CE-CT contrast-enhanced computed tomography

\* In brackets: range size of the lesions (mm)

**Fig. 1** Neuroendocrine tumor of the pancreatic tail unseen by  $^{111}\text{In}$ -pentetreotide single-photon emission computed tomography/computed tomography (a, axial image) but depicted (arrows) with  $^{68}\text{Ga}$ -DOTA-TOC positron emission tomography/computed tomography (b, axial image), with contrast-enhanced computed tomography (c, axial image in arterial phase) and magnetic resonance imaging (d, T1-weighted image after gadolinium injection in arterial phase)



### Detection of extra-abdominal MEN1 tumors

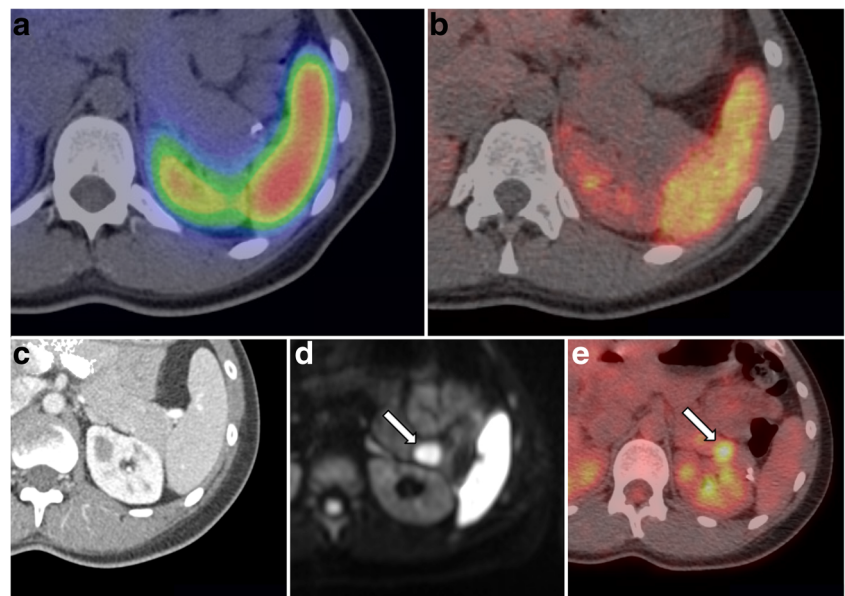
The  $^{68}\text{Ga}$ -DOTA-TOC PET/CT detected three SRS negative meningiomas that were confirmed using complementary MRI (P6, P18, P19).  $^{68}\text{Ga}$ -DOTA-TOC PET/CT also depicted a 14-mm bronchial carcinoid that was not seen during unblinded analysis of CE-CT (P19) (Fig. 3). A grade 3 thymic neuroendocrine carcinoma of 55 mm in size was identified with  $^{68}\text{Ga}$ -DOTA-TOC PET/CT, SRS and CE-CT (P2).

### Discussion

Detection of dpNETs at an early stage, accurate size measurement, and regular monitoring are essential for the

management of MEN1. Multiphase CE-CT and CE-MRI are commonly used to detect dpNETs in MEN1 patients with roughly similar diagnostic performances [3]. Their main drawbacks are their limitation in detecting very small lesions [18]. EUS is considered the most sensitive and precise imaging technique for measurement of dpNETs size [18]. However, EUS is more operator-dependent than cross-sectional imaging and may perform less well for the left portion of the pancreas [19]. Elsewhere, the pathological significance of NF lesions of less than 10 mm is debatable and, importantly, EUS is cumbersome and invasive because it requires general anesthesia. SRS has proved to be effective for visualizing dpNETs [3, 5, 20, 21] and, coupled to SPECT, has the advantage of whole-body scanning, which allows detection of extra-abdominal lesions and metastases. The main

**Fig. 2** Rapidly growing neuroendocrine tumor of the pancreatic tail unseen with  $^{111}\text{In}$ -pentetreotide single-photon emission computed tomography/computed tomography (a, axial image) nor with  $^{68}\text{Ga}$ -DOTA-TOC positron emission tomography/computed tomography (b, axial image) and contrast-enhanced computed tomography (c, axial image in arterial phase) but depicted (arrows) by magnetic resonance imaging (d, diffusion-weighted image after gadolinium injection in arterial phase) with focal intense uptake of  $^{18}\text{F}$ -FDG positron emission tomography/computed tomography (e, axial image)



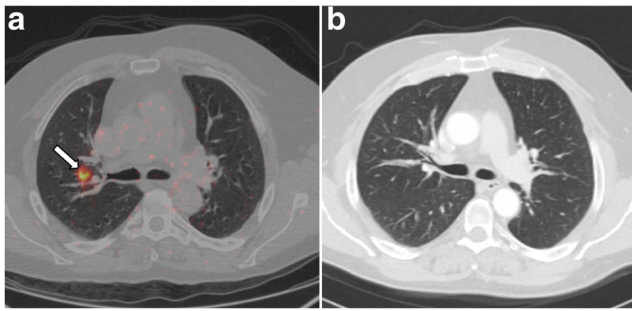


**Fig. 3** Bronchial neuroendocrine tumor depicted by  $^{68}\text{Ga}$ -DOTA-TOC positron emission tomography/computed tomography (**a**, axial image) but unseen with contrast-enhanced computed tomography (**b**, axial image in arterial phase)

limitations of SRS are related to variable expression of  $\text{SST}_2\text{R}$  amongst dpNETs, hepato-biliary elimination of the tracer, which interferes with the interpretation of abdominal images and size of tumors [8]. Due to the high energy of the  $\gamma$  rays of  $^{111}\text{In}$  and partial volume effect in small tumors combined with the intrinsically low resolution of the gamma camera, small tumors (<10 mm in size) are rarely detected by SRS. Also, because of low resolution of SRS imaging, unicus physiological uptake is difficult to differentiate from pathological findings. In the last few years, studies using new high-affinity somatostatin analogs radiolabeled with  $^{68}\text{Ga}$  for PET/CT imaging have emerged. They have shown a higher rate of lesion identification than is achieved with SRS [8–10, 22, 23]. However, to date, limited information is available concerning the accuracy of these new functional imaging tools in the specific situation of MEN1. Two studies conducted with  $^{68}\text{Ga}$ -DOTA-TOC PET/CT or  $^{68}\text{Ga}$ -DOTA-Nal<sup>3</sup>-Octreotide ( $^{68}\text{Ga}$ -DOTA-NOC) PET/CT in a very limited number of MEN-1 patients [11, 12] suffer from major limitations such as a retrospective design and lack of comparison with SRS and multiphase CE-CT. Only one prospective comparative study, assessing the performance and usefulness of  $^{68}\text{Ga}$ -DOTA-TATE PET/CT in 26 MEN-1 patients, is currently available [13]. Therefore, the present work is the largest prospective and head-to-head comparative study assessing the accuracy of  $^{68}\text{Ga}$ -DOTA-TOC PET/CT in MEN1 patients and should be of value.

Patients of our cohort were selected consecutively during regular follow-up and the distribution of dpNETs including a majority of NF dpNETs followed by gastrinomas is representative of the MEN1 spectrum [3]. One limitation of our study is the absence of insulinoma, a tumor that frequently lacks significant  $\text{SST}_2\text{R}$  [24]. Interestingly, dpNETs in our cohort exhibited small size ( $10.4 \pm 7.3$  mm) and only one patient (P6) was treated for a metastatic intermediate-grade pancreatic NET. Of note, the dpNETs phenotype of our cohort differs significantly from the prospective study of Sadowski et al. [13] in which the majority of patients harbored a metastatic disease. Also, the aim of our study was to detect more widely

dpNETs in MEN1 patients whereas the prospective study of Lastoria et al. evaluate the diagnostic performance of  $^{68}\text{Ga}$ -DOTA-TATE PET/CT for detection of pancreatic NET only in MEN1 patients without comparison to SRS [14]. Although our study does not enable the evaluation of  $^{68}\text{Ga}$ -DOTA-TOC PET/CT accuracy for the staging of malignant dpNETs, a goal that was outside the scope of our study. However, it allows the assessment of the performance of imaging tools in a screening perspective for MEN1-related dpNETs.

Our results are in accordance with previous studies conducted in sporadic dpNETs and confirm that the diagnostic performance of  $^{68}\text{Ga}$ -DOTA-TOC PET/CT is clearly superior to that of SRS [9, 10, 23]. Similar findings have recently been reported by Sadowski et al. using  $^{68}\text{Ga}$ -DOTA-TATE PET/CT [13]. More specifically, our study shows that  $^{68}\text{Ga}$ -DOTA-TOC PET/CT is able to depict small lesions of less than 10 mm in size, which were not seen using SRS, enabling a more complete screening of dpNETs. The relatively poor performance of SRS in our cohort, as compared to a 50 to 100 % sensitivity reported in the literature, is probably related to the limited size of most tumors [25]. Elsewhere,  $^{68}\text{Ga}$ -DOTA-TOC PET/CT provided a better characterization of the lesions unseen with cross-sectional imaging. Indeed nine tumors > 10 mm in size and SRS negative were clearly visualized using  $^{68}\text{Ga}$ -DOTA-TOC PET/CT. Therefore, in such SRS negative cases, the improvement in tumor characterization provided by  $^{68}\text{Ga}$ -DOTA-TOC PET/CT may prevent the necessity of performing complementary investigations such as biopsy,  $^{18}\text{F}$ -FDG PET/CT, or more frequent regular follow-up.

The sensitivity of  $^{68}\text{Ga}$ -DOTA-TOC PET/CT also compares well with that of CE-CT (76 and 60 %, respectively, in a per-lesion analysis). Interestingly,  $^{68}\text{Ga}$ -DOTA-TOC PET/CT helped to identify 15 dpNETs unseen with blinded analysis of CE-CT but depicted after unblinded re-analysis. Conversely, 13 dpNETs unseen with  $^{68}\text{Ga}$ -DOTA-TOC PET/CT were identified by CE-CT. However, these FN corresponded to ten small lesions < 12 mm in size, and to  $^{18}\text{F}$ -FDG PET/CT-positive peripancreatic metastatic LN and liver metastases of a grade 3 pancreatic NET (P6).  $\text{SST}_2\text{R}$  expression was described to decrease as the histological grade of dpNETs increases, and there is evidence that, similarly to SRS, new somatostatin analog PET tracers are of limited value in intermediate and high-grade tumors while  $^{18}\text{F}$ -FDG PET is more appropriate [26–28]. Similar considerations may explain the negative findings in the patient P12, with  $^{18}\text{F}$ -FDG PET positive rapidly growing pancreatic lesions associated with LN.

Since EUS is considered to be the most sensitive imaging tool for detecting small dpNETs [3, 18] and not performed in a systematic fashion in all 19 patients, the true sensitivity of  $^{68}\text{Ga}$ -DOTA-TOC PET/CT in our cohort may be overestimated. However, apart from patients with

intermediate or advanced-grade dpNETs, the lesions missed by both  $^{68}\text{Ga}$ -DOTA-TOC PET/CT and CE-CT in asymptomatic individuals are probably of small size and of questionable clinical significance.

Importantly,  $^{68}\text{Ga}$ -DOTA-TOC PET/CT provided a complete mapping of the disease and identified several MEN1 extra-abdominal-related tumors including three meningiomas unseen by SRS and a bronchial NET that was missed by blinded analysis of CE-CT.

As all  $^{68}\text{Ga}$ -DOTA-TOC PET/CT images were confirmed by unblinded analysis and complementary investigations, our study suggests the excellent specificity of  $^{68}\text{Ga}$ -DOTA-TOC PET/CT. Indeed, no FP was recorded in our series. However, the very specific binding of  $^{68}\text{Ga}$ -DOTA-TOC may lead to misinterpretation of tracer accumulation, as described in previous studies, and should be correlated with anatomical imaging findings for accurate interpretation. Acquisition with contrast-enhanced perfusion for CT may also improve  $^{68}\text{Ga}$ -DOTA-TOC PET/CT to localize dpNETs [23, 29]. A clear limitation of our study to assess the specificity of  $^{68}\text{Ga}$ -DOTA-TOC PET/CT is that only pathological examination of surgical specimens can confirm the diagnosis of dpNETs and provide accurate information concerning their real size and histological grade. However, and similarly to the previously published studies in the specific context of MEN1 [11–13], this option was not possible in small lesions for ethical reasons in the context of the restricted surgical indications in MEN1 patients [3]. Interestingly, only a few small LN identified with  $^{68}\text{Ga}$ -DOTA-TOC PET/CT were recorded as false positives after histological examination [13].

In conclusion, in our series,  $^{68}\text{Ga}$ -DOTA-TOC PET/CT demonstrates excellent sensitivity and a real superiority compared to SRS. In addition,  $^{68}\text{Ga}$ -DOTA-TOC PET/CT proved to be helpful for complete mapping of MEN1 disease. Owing to its diagnostic superiority, improved convenience for the patient as 1-day imaging, lower risk of accumulation of radiation in the kidneys compared to SRS [30] and potentially lower cost [31],  $^{68}\text{Ga}$ -DOTA-TOC PET/CT should replace SRS in the investigation of MEN1 patients. Further studies are needed to precisely evaluate its performance in case of insulinomas. Whether the slight difference between  $^{68}\text{Ga}$ -DOTA-TATE and  $^{68}\text{Ga}$ -DOTA-NOC binding affinity to SST<sub>2</sub>R translates into clinical impact, following functional imaging is debatable [32]. Somatostatin agonists radiolabeled with long-lived positron emitters, such as  $^{64}\text{Cu}$ -DOTA-TATE [33], and somatostatin antagonists radiolabeled with  $^{68}\text{Ga}$  are also subject of major interest [34]. Finally, other neuropeptides, such as radiolabeled glucagon-like peptide 1 (GLP-1) analogues or glucose-dependent insulinotropic polypeptide analogues might also improve management of dpNETs that are somatostatin-receptor negative [35].

Our study was not designed to establish the ideal imaging strategy for dpNETs in MEN1 patients. However, as accurate

measurement and functional characterization of all dpNETs are important goals in MEN1 management, we recommend the use of a combination of  $^{68}\text{Ga}$ -DOTA-TOC PET/CT and complementary sensitive morphological imaging such as multiphase CE-CT, EUS, or MRI for the detection of MEN1-related dpNETs.

Although EUS in trained hands is probably the most sensitive imaging technique to detect very small pancreatic tumors (often quite smaller than 1 cm), the clinical significance of such tumors in asymptomatic individuals is debatable, and the availability of expert endoscopists is limited. Thus, in the absence of clinical or biological features suggesting the presence of insulinomas, our study and recent data from the literature suggest that  $^{68}\text{Ga}$ -DOTA-TOC PET/CT (using CE-CT) could be recommended as the standard for screening of GEP-NET in MEN1 patients.

**Acknowledgments** We thank Dr. F. Debordeaux for participation in quality controls and preparation of  $^{111}\text{In}$ -pentetreotide and Mrs. C. Blair for grammatical revision of the manuscript. This study has been funded by “La Ligue contre le Cancer” and was achieved within the context of the Laboratory of Excellence TRAIL ANR-10-LABX-57. The authors declare that they have no conflicts of interest.

**Compliance with ethical standards** All procedures performed in studies involving human participants were in accordance with the ethical standards of the institutional and/or national research committee and with the 1964 Helsinki Declaration and its later amendments or comparable ethical standards.

**Financial support** This work was funded by La Ligue contre le Cancer and was achieved within the context of the Laboratory of Excellence TRAIL ANR-10-LABX-57.

## References

- Chandrasekharappa SC, Guru SC, Manickam P, Olufemi SE, Collins FS, Emmert-Buck MR, et al. Positional cloning of the gene for multiple endocrine neoplasia-type 1. *Science*. 1997;276(5311):404–7.
- Machens A, Schaaf L, Karges W, Frank-Raue K, Bartsch DK, Rothmund M, et al. Age-related penetrance of endocrine tumours in multiple endocrine neoplasia type 1 (MEN1): a multicentre study of 258 gene carriers. *Clin Endocrinol*. 2007;67(4):613–22.
- Thakker RV, Newey PJ, Walls GV, Bilezikian J, Dralle H, Ebeling PR, et al. Clinical practice guidelines for multiple endocrine neoplasia type 1 (MEN1). *J Clin Endocrinol Metab*. 2012;97(9):2990–3011.
- Goudet P, Murat A, Binquet C, Cardot-Bauters C, Costa A, Ruzsiewicz P, et al. Risk factors and causes of death in MEN1 disease. A GTE (Groupe d’Etude des Tumeurs Endocrines) cohort study among 758 patients. *World J Surg*. 2010;34(2):249–55.
- Pieterman CRC, Conemans EB, Dreijerink KMA, de Laat JM, Timmers HTM, Vriens MR, et al. Thoracic and duodenopancreatic neuroendocrine tumors in multiple endocrine neoplasia type 1: natural history and function of menin in tumorigenesis. *Endocr Relat Cancer*. 2014;21(3):R121–42.

6. Öberg KE, Reubi JC, Kwekkeboom DJ, Krenning EP. Role of somatostatins in gastroenteropancreatic neuroendocrine tumor development and therapy. *Gastroenterology*. 2010;139(3):742–53.e1.
7. Johnbeck CB, Knigge U, Kjær A. PET tracers for somatostatin receptor imaging of neuroendocrine tumors: current status and review of the literature. *Future Oncol*. 2014;10(14):2259–77.
8. Kowalski J, Henze M, Schuhmacher J, Macke H, Hofmann M, Haberkorn U. Evaluation of positron emission tomography imaging using  $^{68}\text{Ga}$ -DOTA-DPhe<sup>1</sup>-Tyr<sup>3</sup>-octreotide in comparison to  $^{111}\text{In}$ -DTPAOC SPECT. First results in patients with neuroendocrine tumors. *Mol Imaging Biol*. 2003;5(1):42–8.
9. Buchmann I, Henze M, Engelbrecht S, Eisenhut M, Runz A, Schäfer M, et al. Comparison of  $^{68}\text{Ga}$ -DOTATOC PET and  $^{111}\text{In}$ -DTPAOC (Octreoscan) SPECT in patients with neuroendocrine tumours. *Eur J Nucl Med Mol Imaging*. 2007;34(10):1617–26.
10. Gabriel M, Decristoforo C, Kandler D, Dobrozemsky G, Heute D, Uprimny C, et al.  $^{68}\text{Ga}$ -DOTA-Tyr<sup>3</sup>-octreotide PET in neuroendocrine tumors: comparison with somatostatin receptor scintigraphy and CT. *J Nucl Med*. 2007;48(4):508–18.
11. Froeling V, Elgeti F, Maurer M, Scheurig-Muenkler C, Beck A, Kroencke T, et al. Impact of Ga-68 DOTATOC PET/CT on the diagnosis and treatment of patients with multiple endocrine neoplasia. *Ann Nucl Med*. 2012;26(9):738–43.
12. Sharma P, Mukherjee A, Karunanithi S, Naswa N, Kumar R, Ammini AC, et al. Accuracy of  $^{68}\text{Ga}$  DOTANOC PET/CT imaging in patients with multiple endocrine neoplasia syndromes. *Clin Nucl Med*. 2015;40(7):e351–6.
13. Sadowski SM, Millo C, Cottle-Delisle C, Merkel R, Yang LA, Herscovitch P, et al. Results of  $^{68}\text{Ga}$ -DOTATATE PET/CT scanning in patients with multiple endocrine neoplasia Type 1. *J Am Coll Surg*. 2015;221(2):509–17.
14. Lastoria S, Marciello F, Faggiano A, Aloj L, Caracò C, Aurilio M et al. Role of  $^{68}\text{Ga}$ -DOTATATE PET/CT in patients with multiple endocrine neoplasia type 1 (MEN1). *Endocrine*. 2015.
15. Velikyan I, Beyer GJ, Langstrom B. Microwave-supported preparation of  $^{68}\text{Ga}$  bioconjugates with high specific radioactivity. *Bioconjug Chem*. 2004;15(3):554–60.
16. Morgat C, Mazère J, Fernandez P, Buj S, Vimont D, Schulz J, et al. A phantom-based method to standardize dose-calibrators for new  $\beta^+$ -emitters. *Nucl Med Commun*. 2015;36(2):201–6.
17. Bombardieri E, Ambrosini V, Aktolun C, Baum R, Bishof-Delaloye A, Del Vecchio S, et al.  $^{111}\text{In}$ -pentetreotide scintigraphy: procedure guidelines for tumour imaging. *Eur J Nucl Med Mol Imaging*. 2010;37(7):1441–8.
18. van Asselt SJ, Brouwers AH, van Dullemen HM, van der Jagt EJ, Bongaerts AHH, Kema IP, et al. EUS is superior for detection of pancreatic lesions compared with standard imaging in patients with multiple endocrine neoplasia type 1. *Gastrointest Endosc*. 2015;81(1):159–67.e2.
19. Barbe C, Murat A, Dupas B, Ruzniewski P, Tabarin A, Vullierme M-P, et al. Magnetic resonance imaging versus endoscopic ultrasonography for the detection of pancreatic tumours in multiple endocrine neoplasia type 1. *Dig Liver Dis*. 2012;44(3):228–34.
20. Kwekkeboom DJ, Krenning EP, Scheidhauer K, Lewington V, Lebtahi R, Grossman A, et al. ENETS consensus guidelines for the standards of care in neuroendocrine tumors: somatostatin receptor imaging with  $^{111}\text{In}$ -pentetreotide. *Neuroendocrinology*. 2009;90(2):184–9.
21. Krausz Y, Keidar Z, Kogan I, Even-Sapir E, Bar-Shalom R, Engel A, et al. SPECT/CT hybrid imaging with  $^{111}\text{In}$ -pentetreotide in assessment of neuroendocrine tumours. *Clin Endocrinol (Oxf)*. 2003;59(5):565–73.
22. Ambrosini V, Campana D, Tomassetti P, Fanti S.  $^{68}\text{Ga}$ -labelled peptides for diagnosis of gastroenteropancreatic NET. *Eur J Nucl Med Mol Imaging*. 2012;39(S1):52–60.
23. Schreiter NF, Bartels A-M, Froeling V, Steffen I, Pape U-F, Beck A, et al. Searching for primaries in patients with neuroendocrine tumors (NET) of unknown primary and clinically suspected NET: Evaluation of Ga-68 DOTATOC PET/CT and In-111 DTPA octreotide SPECT/CT. *Radiol Oncol*. 2014;48(4):339–47.
24. Bertherat J, Tenenbaum F, Perlemoine K, Videau C, Alberini JL, Richard B, et al. Somatostatin receptors 2 and 5 are the major somatostatin receptors in insulinomas: an in vivo and in vitro study. *J Clin Endocrinol Metab*. 2003;88(11):5353–60.
25. Scarsbrook AF, Thakker RV, Wass JAH, Gleeson FV, Phillips RR. Multiple endocrine neoplasia: spectrum of radiologic appearances and discussion of a multitechnique imaging approach. *RadioGraphics*. 2006;26(2):433–51.
26. Abgral R, Leboulleux S, Déandris D, Aupérin A, Lumbroso J, Dromain C, et al. Performance of  $^{18}\text{F}$ -fluorodeoxyglucose-positron emission tomography and somatostatin receptor scintigraphy for high Ki67 ( $\geq 10\%$ ) well-differentiated endocrine carcinoma staging. *J Clin Endocrinol Metab*. 2011;96(3):665–71.
27. Squires III M, Volkan Adsay N, Schuster D, Russell M, Cardona K, Delman K, et al. Octreoscan versus FDG-PET for neuroendocrine tumor staging: a biological approach. *Ann Surg Oncol*. 2015;22(7):2295–301.
28. Garin E, Le Jeune F, Devillers A, Cuggia M, de Lajarte-Thirouard A-S, Bourriel C, et al. Predictive value of  $^{18}\text{F}$ -FDG PET and somatostatin receptor scintigraphy in patients with metastatic endocrine tumors. *J Nucl Med*. 2009;50(6):858–64.
29. Ruf J, Schiefer J, Furth C, Kosiek O, Kropf S, Heuck F, et al.  $^{68}\text{Ga}$ -DOTATOC PET/CT of neuroendocrine tumors: spotlight on the CT phases of a triple-phase protocol. *J Nucl Med*. 2011;52(5):697–704.
30. Eberlein U, Lassmann M. Dosimetry of  $^{68}\text{Ga}$ -labeled compounds. *Appl Radiat Isot*. 2013;76:70–4.
31. Schreiter N, Brenner W, Nogami M, Buchert R, Huppertz A, Pape U-F, et al. Cost comparison of  $^{111}\text{In}$ -DTPA-octreotide scintigraphy and  $^{68}\text{Ga}$ -DOTATOC PET/CT for staging enteropancreatic neuroendocrine tumours. *Eur J Nucl Med Mol Imaging*. 2012;39(1):72–82.
32. Yang J, Kan Y, Ge BH, Yuan L, Li C, Zhao W. Diagnostic role of Gallium-68 DOTATOC and Gallium-68 DOTATATE PET in patients with neuroendocrine tumors: a meta-analysis. *Acta Radiol*. 2014;55(4):389–98.
33. Pfeifer A, Knigge U, Binderup T, Mortensen J, Oturai P, Loft A, et al.  $^{64}\text{Cu}$ -DOTATATE PET for neuroendocrine tumors: a prospective head-to-head comparison with  $^{111}\text{In}$ -DTPA-Octreotide in 112 patients. *J Nucl Med*. 2015;56(6):847–54.
34. Gjinj M, Zhang H, Waser B, Cescato R, Wild D, Wang X, et al. Radiolabeled somatostatin receptor antagonists are preferable to agonists for in vivo peptide receptor targeting of tumors. *Proc Natl Acad Sci U S A*. 2006;103(44):16436–41.
35. Morgat C, Mishra AK, Varshney R, Allard M, Fernandez P, Hindie E. Targeting neuropeptide receptors for cancer imaging and therapy: perspectives with bombesin, neurotensin, and neuropeptide-Y receptors. *J Nucl Med*. 2014;55:1650–7.